JOURNAL OF PROPULSION AND POWER
Vol. 23, No. 6, November–December 2007

Electromagnetic Pumps for Liquid Metal-Fed Electric Thrusters

Kurt A. Polzin* and Thomas E. Markusic†
NASA Marshall Space Flight Center, Huntsville, Alabama 35812

DOI: 10.2514/1.30819

Prototype designs of two separate pumps for use in electric propulsions systems with liquid lithium and bismuth propellants are presented. Both pumps are required to operate at elevated temperatures, and the lithium pump must additionally withstand the corrosive nature of the propellant. Compatibility of the pump materials and seals with lithium and bismuth were demonstrated through proof-of-concept experiments followed by postexperiment visual inspections. The pressure rise produced by the bismuth pump was found to be linear with input current and ranged from 0–9 kPa for corresponding input current levels of 0–30 A, showing good quantitative agreement with theoretical analysis.

Nomenclature

$\boldsymbol{B}$, B	=	magnetic induction, T
$\boldsymbol{F}$, F	=	force, N
I	=	pump current, A
I_{sp}	=	specific impulse, s
$\boldsymbol{j}$	=	pump current density, A/m^2
l	=	pump channel length, m
P	=	pressure, Pa
s	=	pump channel height, m
t	=	time, s
w	=	pump channel width, m
x	=	integration variable, m

I. Introduction

METALLIC propellants have been used in almost all major categories of electric propulsion (EP) devices. These have included lithium-fed arcjets [1] and magnetoplasmadynamic (MPD) thrusters [2], mercury- [3,4], cesium- [5,6], and indium-fed [7] electrostatic thrusters (both ion engines and field emission electric propulsion), and bismuth-fed Hall thrusters [8–10].

Present interest in liquid-metal-fed electric propulsion systems has been spurred by recently published data showing promising performance in systems operating on liquid-metal propellants. For example, a lithium-fed MPD thruster operating at 500 kW demonstrated over 50% efficiency with 500 h of electrode erosion-free operation [11]. Also, a bismuth-fed Hall thruster demonstrated high-power operation (140 kW) while maintaining high performance (8000s I_{sp} at greater than 70% anode efficiency) at 10 kV discharge voltage [8].

The use of a metallic propellant in a plasmathruster can result in systems and logistics-level advantages over gas-fed thrusters. For example, a gas (e.g., supercritical xenon) must be stored in high-pressure tanks to obtain a high propellant density, whereas a metallic propellant may be stored as either a solid or dense liquid, implying a reduction in the structural mass of the tank. In addition, vaporized metallic propellants can be condensed using simple, water-cooled plates to obtain equivalent pumping speeds of millions of liters per second, making high-power, long-duration tests possible in present vacuum facilities.

Received 4 March 2007; revision received 15 June 2007; accepted for publication 31 July 2007.

*Research Scientist, Nuclear Systems Branch, Propulsion Systems Department; kurt.a.polzin@nasa.gov. Senior Member AIAA.

†Research Scientist; currently Propulsion Test Manager, Space Exploration Technologies, Inc., El Segundo, CA 90245.

An important component in a liquid-metal-fed thruster is the mechanism that applies pressure to force propellant from a reservoir to the thruster. Although there are many ways to pressurize the propellant, we chose to develop electromagnetic (EM) pumps to exploit the conductive nature of the propellant. The corrosive nature of the liquid lithium and bismuth environments severely restricted the range of materials that could be used. Both electrically insulating and conducting materials were employed in the construction of our pumps, which led to the additional challenge of joining and sealing vastly differing materials. To our knowledge, this paper represents the first discussion of EM pumps where the main body was fabricated from an insulating material. Electromagnetic pump designs for both a lithium-fed and a bismuth-fed system are described, and both qualitative and quantitative data are presented to demonstrate the performance of the pumps.

In Sec. II, we briefly review liquid-metal EM pumping technologies, specifically highlighting instances in which EM pumps have been used in electric propulsion systems. We describe the general theoretical aspects of pump design and provide design details for both the lithium and bismuth pumps in Sec. III. The experiments performed to demonstrate pump operation and quantify performance are discussed in Sec. IV. Results obtained from our experiments are presented in Sec. V.

II. Background

Much effort was expended on the development of EM pump technologies in the mid-1950s for use in liquid-metal cooling loops for nuclear fission reactors [12–14]. This technology was widely deployed or considered for deployment in both ground-based [15] and space-based [16] reactor systems. Additional uses for EM pumps include the movement and control of seawater, molten metals, and various other conducting liquid metals employed in laboratory research [17].

For propellant control in electric propulsion applications, EM pumps possess several advantages over conventional mechanical pumps. They have no moving parts, thus eliminating mechanical friction losses and the need for bearings and rotating seals. This is especially advantageous if the propellant is highly reactive. Propellant pressurization is controlled by adjusting the input current and, as a result, control can be executed with a high degree of fidelity over the entire pump operating range. EM pumps are reliable, possessing no parts that are particularly failure-prone, and can be scaled to small sizes. Consequently, these pumps should prove well suited as flow controllers in electric propulsion feed systems.

Although EM pumps have not been used as the primary propellant feeding mechanism in electric thrusters, they have been used as an auxiliary system in conjunction with elastic diaphragms in mercury ion engines [3,4,18]. In these systems, the EM pump acted as a mechanism to provide fine-adjustment of the mercury pressure head

at the propellant vaporizer. One such pump produced a pressure differential of 0.6 atm at a 20 A current level [4].

The primary designs used for electromagnetically pumping liquid metals are direct-current (DC) and alternating-current (AC) conduction pumps and linear induction pumps. In conduction pumps, current is directly passed through the fluid and a magnetic field is applied perpendicular to both the current and flow vectors. In induction pumps, the current and magnetic field in the fluid are both induced by externally flowing currents that are time varying. The external currents oscillate so as to drive an induced, travelling magnetic wave through the fluid. We chose to develop DC conduction pumps for EP applications due to their relatively simple and easily scalable design.

III. Engineering Design

We proceed with a brief discussion of the theoretical aspects of DC EM conduction pump design and then describe the two EM pumps constructed for this study.

A. EM Pump Theory

An idealized schematic of a DC conduction pump is presented in Fig. 1. The liquid metal flows though a channel of width w, length l, and height s. The magnetic field B and current I are perpendicular to the flow (and each other) and are uniform over the indicated faces. When current flows between the electrodes, a Lorentz body force is exerted on the fluid in the direction of the flow vector. Integration of the body force is written as

$$|\boldsymbol{F}| = \int \boldsymbol{j} \times \boldsymbol{B}\, \mathrm{d}^3x \tag{1}$$

where $\boldsymbol{j}$ is the current density (equal in magnitude to $I/(ls)$ when $|\boldsymbol{j}|$ is uniform). Performing the integration yields

$$F = \frac{I}{ls} Blsw = IBw \tag{2}$$

for uniform $\boldsymbol{B}$ and $\boldsymbol{j}$. The force causes a fluid pressure increase to develop which is equal to

$$P = \frac{F}{sw} = \frac{IB}{s} \tag{3}$$

In Eq. (3), the pressure developed by the pump is only a function of the channel height, magnetic field strength, and total current. Material properties, specifically the conductivity of the fluid, are important only when considering the electric potential required to drive the current I through the pump. The relationship in Eq. (3) is plotted in Fig. 2 as a function of the parameters B/s and I. In practice, the maximum value of B/s that can be achieved is $\sim$10 T/cm. If we limit the current to below $\sim$100 A to avoid excessive Ohmic heating losses, the pump pressure that can be developed in an optimized pump is roughly 10^5 Pa (1 atm).

B. Lithium Pump Design

In the present study, we chose to fabricate our lithium EM pump from ceramic to minimize stray conduction losses. To our knowledge, this is the first use of an insulating material for the body of an alkali metal EM pump. Although the previous analysis shows that the current required to attain a given pump pressure decreases for increasing values of B/s, the materials employed place certain practical limits on the maximum attainable value. The brittle nature of ceramic materials led to the choice of a relatively large value for s to minimize the potential for cracking in the walls separating the magnets from the fluid flow channel.

Aluminum nitride (AlN) was chosen as the insulating body material and, although it is difficult to machine, it can survive the corrosive nature of the molten lithium environment ($\geq$ 250 C). A major pump fabrication issue was the method by which metallic electrodes and liquid feed lines were joined to the ceramic body. The problem was made worse by the fact that the interface must be

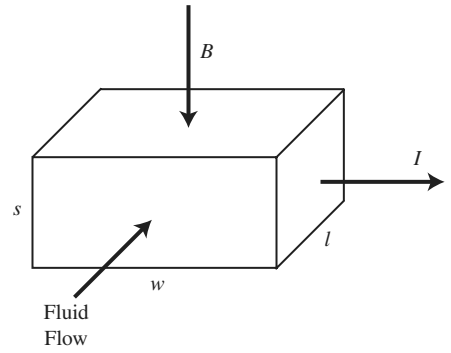

Fig. 1 Idealized schematic of an electromagnetic pump.

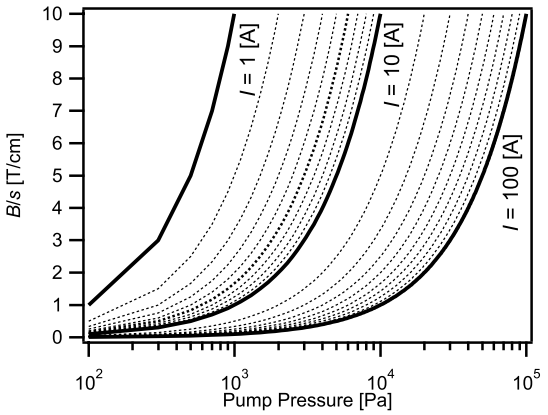

Fig. 2 B/s ratio as a function of desired pump pressure for varying values of pump current.

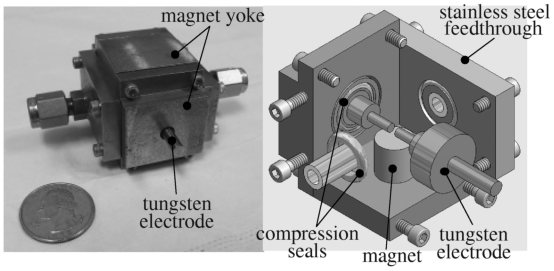

a) b)

Fig. 3 Lithium EM pump: a) photograph of assembled pump (with U.S. quarter to show relative scale), b) CAD drawing with pump body removed to show inner detail.

hermetically sealed to avoid liquid leaks. We chose to employ Inconel c-ring seals (compression gaskets) at all sealed joints.

The lithium EM pump was composed of the following additional components: tungsten electrodes, 316L stainless steel liquid feed lines, samarium cobalt magnets, and an iron magnetic yoke. The yoke, electrodes, and feed line end caps were designed to also serve as a means for compressing the c-ring seals. The assembled pump is shown in Fig. 3a and a solid model with the pump body removed to show the inner detail is found in Fig. 3b. The magnet separation in this design was 6.4 mm and the measured value of B was 0.45 T. The magnet employed was much wider than the diameter of the flow channel and much longer than the electrode width. Consequently, we expect the $\boldsymbol{B}$ field is constant over the region where current passes through the liquid metal in agreement with the assumptions made in the derivation of Eq. (3).

C. Bismuth Pump Design

Like the lithium pump, the bismuth EM pump was also fabricated from an insulating material to minimize stray conduction losses.

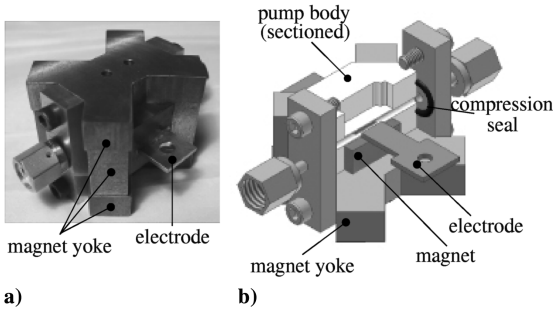

Fig. 4 Bismuth EM pump: a) photograph of assembled pump, b) CAD drawing sectioned to reveal inner detail.

Although molten bismuth at ~300°C is not as corrosive as lithium, it was still a challenge to identify an insulating material that could be used for the pump body. We chose to use glass-mica ceramic (also known as macor) because it is nonreactive at liquid bismuth temperature levels. Relative to the AlN used in the lithium pump, it is also inexpensive and easily machinable. Samarium cobalt magnets were again employed in this pump, but relative ease of machining allowed for a magnet separation (2.9 mm) that was considerably smaller than in the lithium pump case resulting in an on-axis magnetic field strength of 0.64 T. Again, the magnets were significantly larger than the dimensions of the flow channel and electrodes to maintain a constant $\boldsymbol{B}$ field in the pump.

A photograph of the assembled bismuth EM pump is shown in Fig. 4a and a sectioned-view CAD model in Fig. 4b reveals the inner details of the pump's construction. The pump was composed of the following additional components: Inconel electrodes and c-ring compression seals, 316L stainless steel liquid feed lines, and an iron magnet yoke. The electrodes were bonded to the macor body using Ceramabond 569 high-temperature alumina adhesive.

IV. Test Apparatus

In this section, we describe two types of experiments that were conducted to demonstrate EM pump operation, verify the design approach, and quantify pump performance.

A. Open-Loop Apparatus

Qualitative, proof-of-concept experiments were performed using an open-loop flow apparatus. These tests were carried out to demonstrate that the pumps could contain liquid metals at the required operating temperature levels and electromagnetically push the fluids from a reservoir into a catch basin. The flow loops used for the lithium and bismuth pumps are shown in Fig. 5. Because the EM pumps were situated above their respective reservoirs, it was necessary to "prime" the pumps at the beginning of a test by pressurizing the liquid metal in the reservoir using argon. Testing was conducted inside a vacuum chamber to minimize convective heat losses from the system and keep the liquid metals from excessively oxidizing. The setups were mounted on long, thin standoffs and ceramic spacers to minimize the level of conductive cooling. This left radiation as the primary cooling mechanism.

B. Pressure Measurement Apparatus

A test apparatus was constructed to facilitate direct, quantitative measurement of the EM pump pressure as a function of applied current. From Eq. (3) we observe that pressure developed by the pump is independent of the conductive fluid so long as sufficient voltage is available to drive current through the pump. Consequently, we employed liquid gallium as a substitute fluid to eliminate the hazards and difficulties associated with handling and testing lithium and bismuth.

A photograph and schematic illustration of the apparatus used to measure the pressure rise across the pump are shown in Fig. 6. The bottoms of the two liquid metal reservoirs were connected through the EM pump and both reservoirs were initially pressurized using

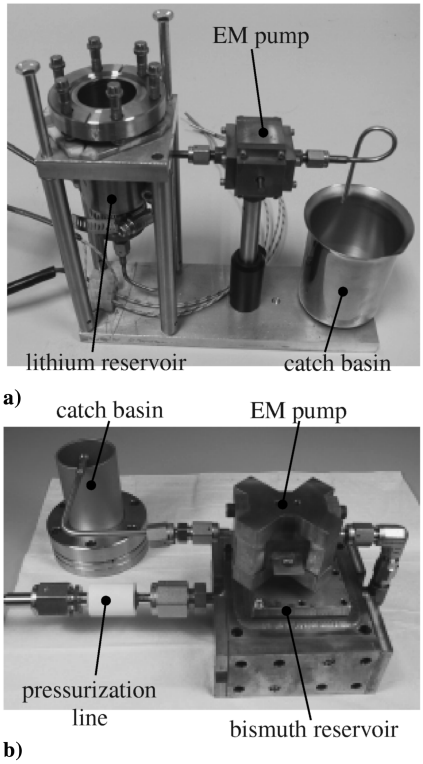

Fig. 5 Photograph of an open-loop test apparatus used for a) lithium, b) bismuth.

argon. Pressure in each reservoir was monitored using an MKS 221 differential capacitance manometer and the valves (V_1, V_2, V_3) in the system allowed for pressurization and evacuation of the reservoirs and pressure equalization between the two reservoirs.

To illustrate the operation of the test apparatus, a notional depiction of the gas pressure readings in each reservoir is presented in Fig. 7. At time t_0, there is no current passing through the pump and the fluid in each reservoir is at an equilibrium level, yielding gas pressures in reservoirs 1 and 2 equal to $P_1(t_0)$ and $P_2(t_0)$, respectively. At time t_1, a fixed, steady current is applied to the EM pump and fluid begins to flow from reservoir 1 to reservoir 2, decreasing the pressure in the former and increasing it in the latter until a new equilibrium is reached at time t_2. Unfortunately, the change in pressure at time t_2 is a composite of the EM pump pressure P_{EM} and the gravitational pressure change (elevation head) associated with the change in the relative heights of the two columns of liquid metal in the reservoirs. Our test apparatus was designed to circumvent this difficulty, using the subsequent steps to eliminate the need to measure any liquid metal height change. Opening valve V_2 at time t_3 further increases the pressure in reservoir 2, forcing the liquid metal back through the pump and into reservoir 1. At time t_4, the liquid metal column heights in the reservoirs are equal to their levels at t_0 and the pressure in reservoir 1 satisfies the condition $P_1(t_4) = P_1(t_0)$. When the fluid column heights return to their initial levels, the excess pressure in reservoir 2 is solely balanced by the pressure applied by the EM pump:

$$P_{\mathrm{EM}} = P_2(t_4) - P_2(t_0) \tag{4}$$

V. Experimental Results

A. Lithium Open-Loop Tests

Approximately 100 g of lithium were loaded into the reservoir of the test apparatus shown in Fig. 5a. The reservoir was heated to ~300°C using a band heater, whereas the tube between the reservoir and the pump was heated using a cartridge heater. The EM pump was not actively heated, relying only on heat conducted through the connecting tube initially and through the tube and the lithium after

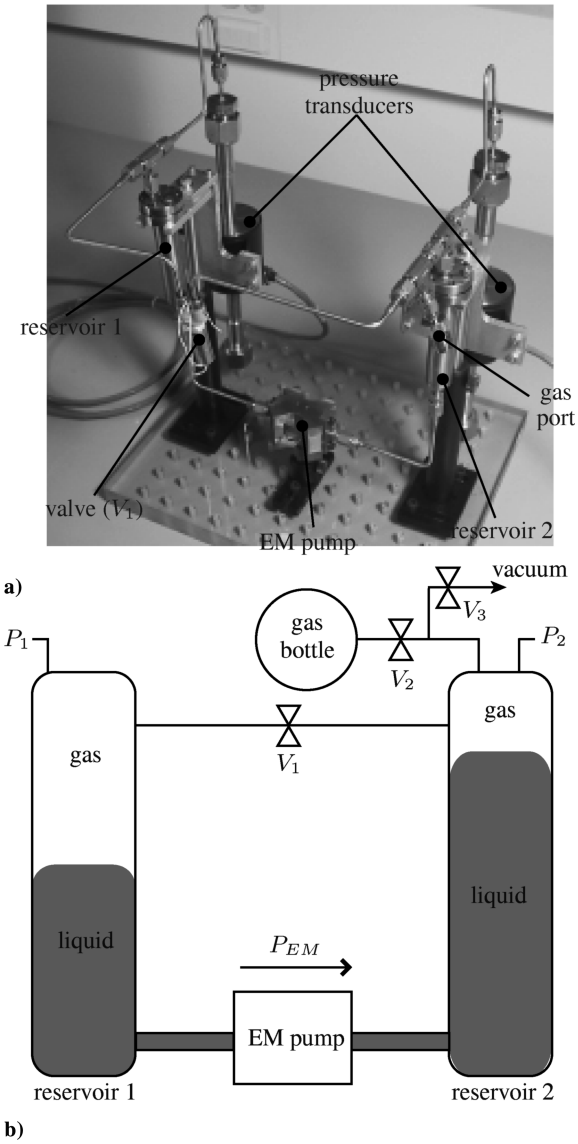

Fig. 6 Pump pressure measurement apparatus: a) photograph, b) schematic.

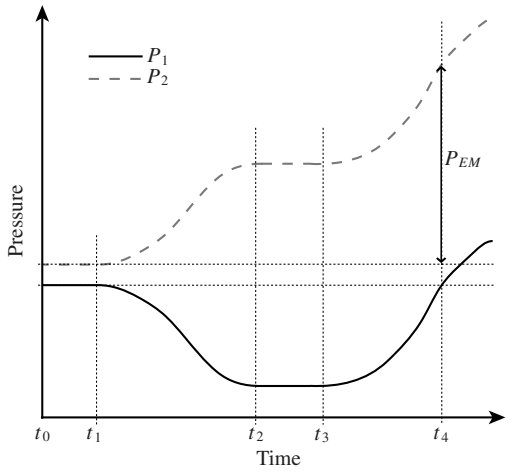

Fig. 7 Notional depiction of the gas pressures in each reservoir of the pump pressure measurement apparatus as a function of time.

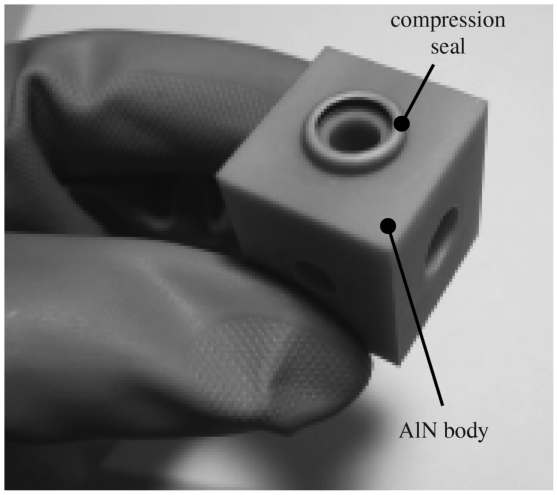

Fig. 8 Lithium EM pump body shown after the open-loop demonstration test.

the pump was primed to reach and maintain a temperature of ∼250°C. Argon gas at a pressure of 15 torr was introduced into the reservoir to prime the pump. After the electrodes in the pump were electrically bridged by liquid lithium, the pump current was set to 20 A. Lithium flow (at a rate of ∼1 g/s) commenced and liquid droplets were expelled into the catch basin. The EM pump was operated with molten lithium for approximately 100 s during the test run, after which time the lithium supply in the reservoir was exhausted. The pump was exposed to liquid and then hot solid lithium for several hours while it cooled to room temperature. It took this long to cool the system owing to the combined thermal inertia of all the components and the limited heat transfer obtained through radiative cooling.

We only performed one test, and so we have no information regarding repeated thermal cycling of the EM pump. However, during that test we did electrically cycle the pump several times by turning the current on and off. The pump was successfully cycled several times to verify the ability to restart pumping. Qualitatively, there did not appear to be an effect on the flow rate as the pump was cycled, but we have no quantitative data regarding the variation of flow rate as a function of pump cycling owing to effects like lithium wetting of the electrodes or clogging of the pump or tube.

Aside from demonstrating electromagnetic pumping with lithium, we also sought to validate the short-term compatibility of our pump materials and sealing techniques with the molten lithium environment (i.e., demonstrate that no immediate problems arose due to our choice of pump materials and seals). After the test run, the pump was disassembled and visually inspected. No evidence of material degradation was observed (see Fig. 8). The AlN body showed no visible signs of cracking or short-term failure and no lithium was evident outside of the compression seals. The metallic components of the pump also appeared to be undamaged. The long-term corrosive effects of liquid lithium on the pump materials and seals were not evaluated, and would require extended life testing that was beyond the scope of the present study.

B. Bismuth Open-Loop Tests

The same test procedure was implemented for open-loop bismuth tests and similar, positive results were obtained. The main difference was that the bismuth reservoir had to be brought to a higher temperature (∼325°C) before flow could be initiated. Several tests (∼10) were performed, with the pump remaining at elevated temperature for several hours during each test. No degradation of the macor or seals was evident through visual inspections after the tests and no leaks were found.

C. EM Pump Pressure Rise

The pressure rise produced by the bismuth EM pump design was evaluated over an applied current range of 10–30 A using the test apparatus shown in Fig. 6, and with liquid gallium substituted for liquid bismuth as discussed in Sec. IV.B. A time history of the raw

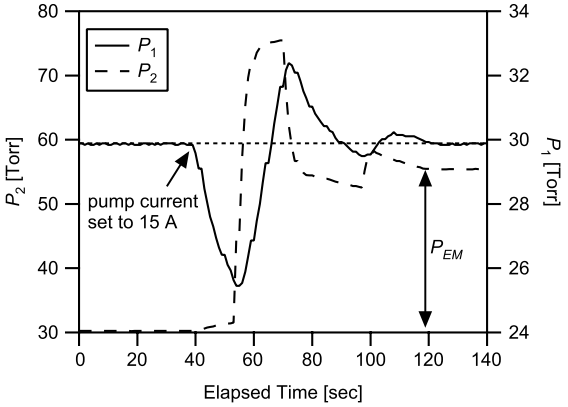

Fig. 9 Raw reservoir pressure data as a function of time obtained using the setup shown in Fig. 6 with the EM pump current set to 15 A at $t = 40$ s using liquid gallium as a working fluid.

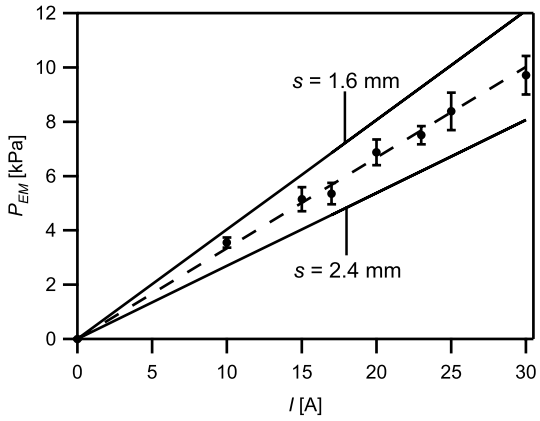

Fig. 10 Measured EM pump pressure vs current (solid lines are theoretical curves computed using Eq. (3) and based on the values of s given, whereas the dashed line represents a linear curve fit of the data).

pressure measurements in the two reservoirs for an applied EM pump current of 15 A is presented in Fig. 9. The results of our testing indicated that the liquid metal had a tendency to "stick" at low flow speeds, possibly due to oxidation layers forming on the gallium surface or reservoir walls impeding wetting and flow. A result of this impediment was that reservoir 1 was unable to return to its initial (pressure) state in a monotonic manner. It was necessary to alternate between overpressurizing and underpressurizing reservoir 2 to maintain liquid flow, which caused the pressure in reservoir 1 to oscillate about the initial pressure with progressively decreasing amplitude. The smallest difference between the high and low values of the pressure in reservoir 2 were used to establish the uncertainty in the measurement of P_{EM}.

The measured values of P_{EM} as a function of pump current for several different trials are presented in Fig. 10. The data show that the pressure developed by the EM pump is linear with current, as indicated by the linear curve fit (dashed line) of the function

$$P_{\mathrm{EM}} = aI \tag{5}$$

where a is the fit coefficient. For the bismuth pump, this value was 336 ± 16 Pa/A. As noted, this coefficient is independent of the type of liquid-metal propellant used. The systematic uncertainties associated with the measurement instruments were small compared with the uncertainty inherent in the measurement procedure, and is therefore not included in the uncertainty analysis.

The pump's theoretical performance can be computed using Eq. (3), but there is some ambiguity in defining the channel height s. The pump was constructed by drilling an axial, 2.4-mm-diam hole through the center, but the electrodes that penetrate through the sides of the pump are only 1.6 mm in height. The actual value of s is dependent on the (unknown) manner in which current distributes itself within the cylindrical channel. It is reasonable to assume that the effective value of s must be somewhere between 1.6 and 2.4 mm in our pump. In Fig. 10 we have plotted theoretical EM pump pressures computed using Eq. (3) for each of these extreme cases. The measured data show good quantitative agreement, lying roughly midway between the two theoretical curves.

The data demonstrate that the bismuth EM pump is capable of delivering a pressure of $\mathcal{O}(10^4)$ Pa at 30 A. Furthermore, the pump is seen to operate at a level consistent with the theoretical maximum performance, implying that losses associated with stray conduction currents are negligible in the present design. Finally, the linearity of the pump pressure data indicate that the effective value of s in the pump is relatively constant (linear scaling of current density in the channel) as input current is increased up to at least 30 A.

VI. Conclusions

The following major results and conclusions are reported in this study. Our EM pump designs were based around central, insulating ceramic bodies, which was a departure from all earlier liquid-metal EM pump work. Material compatibility with liquid lithium led us to design an EM pump around an aluminum nitride body. The pump was fabricated and tested in the relevant environment, and subsequent disassembly of the pump revealed no short-term degradation of the AlN body, stainless steel feed lines, or tungsten electrodes, indicating that the pump would not immediately fail when brought into contact with liquid lithium. The metallic compression seals used to join the conducting and insulating components showed no short-term signs of leakage. An EM pump for use with hot liquid bismuth was fabricated from macor. The relative ease of machinability of macor compared with AlN allowed for a pump design with a much smaller magnet separation than that found in the lithium pump. This resulted in a greater magnetic field in the flow channel. The pump was successfully operated and showed no signs of degradation or leakage after exposure to liquid bismuth over several thermal cycles and $\mathcal{O}(10$ h) of operation. Quantitative measurements of EM pump pressure in the bismuth pump using liquid gallium as a substitute fluid show that the output was linear with current, with a pump pressure of $\sim$10 kPa produced at 30 A. The experimentally measured and theoretically computed pressure values exhibit good quantitative agreement, indicating minimal stray conduction current losses and linear scaling of current density in the channel.

Acknowledgments

We gratefully acknowledge the contributions and support of our research engineer Boris Stanojev and the Marshall Space Flight Center (MSFC) technical support staff: Doug Davenport, Tommy Reid, Doug Galloway, Keith Chavers, and Rondal Boutwell. We also extend our gratitude to Noah Rhys and students Amado DeHoyos, Chris Dodson, and Jeff Gross for their contributions to this work. This work was supported by NASA's Exploration Systems Mission Directorate (Project Prometheus) and funded under contract NNM05AA25C managed by Randy Baggett and NAS7-03001 managed by John Warren.

References

[1] Connolly, D. J., Sovie, R. J., Michels, C. J., and Burkhart, J. A., "Low Environmental Pressure MPD Arc Tests," *AIAA Journal*, Vol. 6, No. 7, 1968, pp. 1271–1276.

[2] Kodys, A. D., Emsellem, G., Cassady, L. D., Polk, J. E., and Choueiri, E. Y., "Lithium Mass Flow Control for High Power Lorentz Force Accelerators," *AIP Conference Proceedings*, Vol. 552, Feb. 2001, pp. 908–915. doi:10.1063/1.1358027

[3] King, H. J., Molitor, J. H., and Kami, S., "System Concepts for a Liquid Mercury Cathode Thruster," AIAA Paper 1967-699, Sept. 1967.

[4] Hyman, J., Jr., Bayless, J. R., Schnelker, D. E., Ward, J. W., and Simpkins, J., "Development of a Liquid-Mercury Cathode Thruster System," *Journal of Spacecraft and Rockets*, Vol. 8, No. 7, 1971, pp. 717–721.

[5] Collett, C. R., Dulgeroff, C. R., and Simpkins, J. M., "Cesium Microthruster System," AIAA Paper 1969-292, March 1969.
[6] Marcuccio, S., Genovese, A., and Andrenucci, M., "Experimental Performance of Field Emission Microthrusters," *Journal of Propulsion and Power*, Vol. 14, No. 5, 1998, pp. 774–781.
[7] Tajmar, M., Genovese, A., and Steiger, W., "Indium Field Emission Electric Propulsion Microthruster Experimental Characterization," *Journal of Propulsion and Power*, Vol. 20, No. 2, 2004, pp. 211–218.
[8] Tverdokhlebov, S. O., Semenkin, A. V., and Polk, J. E., "Bismuth Propellant Option for Very High Power TAL Thruster," AIAA Paper 2002-348, Jan. 2002.
[9] Sengupta, A., Marrese-Reading, C., Cappelli, M., Scharfe, D., Tverdokhlebov, S., Semenkin, S., Tverdokhlebov, O., Boyd, I., Keidar, M., Yalin, A., Surla, V., Markusic, T., and Polzin, K., "An Overview of the VHITAL Program: A Two-Stage Bismuth Fed Very High Specific Impulse Thruster with Anode Layer," *International Electric Propulsion Conference*, Electric Rocket Propulsion Society Paper 2005-238, Oct. 2005.
[10] Wilson, F., "Propulsion and Energy: Electric Propulsion," *Aerospace America*, Vol. 44, No. 12, 2006, pp. 62–63.
[11] Ageyev, V. P., and Ostrovsky, V. G., "High Current Stationary Plasma Accelerator of High Power," *International Electric Propulsion Conference*, Electric Rocket Propulsion Society Paper 93-117, Sept. 1993.
[12] Barnes, A. H., "Direct-Current Electromagnetic Pumps," *Nucleonics*, Vol. 11, No. 1, 1953, pp. 16–21.
[13] Blake, L. R., "Conduction and Induction Pumps for Liquid Metals," *Proceedings of the Institution of Electrical Engineers*, Inst. for Electrical and Electronics Engineers, Paper 2111U, July 1956, pp. 49–63.
[14] Watt, D. A., "Design Of Electromagnetic Pumps For Liquid Metals," *Proceedings of the Institution of Electrical Engineers*, Inst. for Electrical and Electronics Engineers Paper 2763U, Dec. 1958, pp. 94–103.
[15] El-Genk, M. S., and Paramonov, D. V., "An Integrated Model of the TOPAZ-2 Electromagnetic Pump," *Nuclear Technology*, Vol. 108, No. 2, 1994, pp. 171–180.
[16] Polzin, K. A., "Liquid Metal Pump Technologies for Nuclear Surface Power," *Space Nuclear Conference*, American Nuclear Society Paper 2002, June 2007.
[17] Rossow, V. J., "Flow in Direct Current Electromagnetic Pumps," *Reviews of Modern Physics*, Vol. 32, No. 4, 1960, pp. 987–991. doi:10.1103/RevModPhys.32.987
[18] Holcomb, L. B., and Womack, J. R., "Design of a Mercury Propellant Storage and Distribution Assembly," AIAA Paper 1973-1119, Oct. 1973.

E. Choueiri
Associate Editor